RESEARCH ARTICLE

Introgression between highly divergent fungal sister species

Vilde Bruhn Kinneberg[1,2] ⓘ | **Dabao Sun Lü**[1] ⓘ | **David Peris**[1,3] ⓘ | **Mark Ravinet**[4] ⓘ | **Inger Skrede**[1] ⓘ

[1]Section for Genetics and Evolutionary Biology, Department of Biosciences, University of Oslo, Oslo, Norway

[2]Evolution and Paleobiology, Natural History Museum, University of Oslo, Oslo, Norway

[3]Department of Food Biotechnology, Institute of Agrochemistry and Food Technology (IATA), CSIC, Valencia, Spain

[4]School of Life Sciences, University of Nottingham, Nottingham, UK

Correspondence
Vilde Bruhn Kinneberg, Section for Genetics and Evolutionary Biology, Department of Biosciences, University of Oslo, Oslo 0316, Norway.
Email: v.b.kinneberg@nhm.uio.no

Abstract

To understand how species evolve and adapt to changing environments, it is important to study gene flow and introgression due to their influence on speciation and radiation events. Here, we apply a novel experimental system for investigating these mechanisms using natural populations. The system is based on two fungal sister species with morphological and ecological similarities occurring in overlapping habitats. We examined introgression between these species by conducting whole genome sequencing of individuals from populations in North America and Europe. We assessed genome-wide nucleotide divergence and performed crossing experiments to study reproductive barriers. We further used ABBA–BABA statistics together with a network analysis to investigate introgression, and conducted demographic modelling to gain insight into divergence times and introgression events. The results revealed that the species are highly divergent and incompatible in vitro. Despite this, small regions of introgression were scattered throughout the genomes and one introgression event likely involves a ghost population (extant or extinct). This study demonstrates that introgression can be found among divergent species and that population histories can be studied without collections of all the populations involved. Moreover, the experimental system is shown to be a useful tool for research on reproductive isolation in natural populations.

KEYWORDS
ABBA–BABA, demographic modelling, experimental system, ghost introgression, population genomics, *Trichaptum*

1 | INTRODUCTION

Speciation can occur rapidly, changing the course of evolution in a single event, or over a long period of time with gradual shifts from semi-compatible populations to complete divergence (Nosil et al., 2017). When speciation occurs gradually, barriers to gene exchange do not arise immediately and gene flow between diverging populations can be maintained. Consequently, hybrid individuals may form (Harrison & Larson, 2014; Ravinet et al., 2018). If these

hybrids backcross into one of the parental species, a scenario termed introgression (Aguillon et al., 2022; Anderson & Hubricht, 1938), it can result in unique genetic combinations (Stukenbrock, 2016). The amalgamation of genes across lineages can also contribute to the strengthening of barriers to gene exchange. These barriers can arise when selection increases reproductive isolation, a process known as reinforcement (Butlin, 1987). Hybrids can contribute to reinforcement because they often have detrimental gene combinations, resulting in poorer fitness compared to the parental species

(Abbott et al., 2013). Consequently, hybridization can both give rise to beneficial gene combinations which selection can act upon, and at the same time accelerate the divergence process by contributing to reproductive barriers (Abbott et al., 2010).

Hybridization is established as a common event in nature and can lead to the formation of hybrid species (Ackermann et al., 2019; Eberlein et al., 2019; Grant & Grant, 2019; Mallet et al., 2016), as seen in several taxa including plants (e.g., *Senecio* spp.; Hegarty & Hiscock., 2005; Wood et al., 2009), animals (e.g., *Heliconius* butterflies; Mavárez et al., 2006 and *Passer italiae*; Hermansen et al., 2011) and certain fungal groups (e.g., *Saccharomyces* spp.; Langdon et al., 2019 and *Zymoseptoria pseudotritici*; Stukenbrock et al., 2012). Even though hybridization seems to be common in contemporary populations, we do not know the impact it will have on future populations. By studying the genomes of contemporary species with a history of hybridization and introgression, it may be possible to understand how previous interspecific gene exchange have influenced the populations we observe today and infer the future effect of current events.

When taxa have diverged over a long period of time, it can be difficult to discover ancient admixture as genomic signals of introgression can be blurred over macroevolutionary time. Moreover, detection might be difficult due to the deleterious nature of most introgressed genes between divergent species, or the lack of time for introgressed regions to spread in the population if the gene flow is recent (Maxwell et al., 2018). Hence, the evolutionary history of a genus can be complex even though current investigations recover clear and resolved phylogenies (Keuler et al., 2020).

Signs of ancient or low-frequency introgression have been possible to detect using high-throughput sequencing and statistical models (e.g., Crowl et al., 2019; Ravinet et al., 2018). Regions of introgression might constitute small parts of otherwise divergent genomes due to erosion of linkage by recombination coupled with a long period of mostly independent evolution or purifying selection (Cuevas et al., 2022; Martin et al., 2019; Maxwell et al., 2018; Ravinet et al., 2018; Schumer et al., 2018). The retention of specific introgressed regions can, for example, represent adaptational benefits (Racimo et al., 2015), regions of highrecombination rate (Nachman & Payseur, 2012; Ravinet et al., 2018; Schumer et al., 2018), and regions under lower constraint or less purifying selection (Schumer et al., 2016). However, the patterns of introgression can also be difficult to distinguish from mechanisms such as incomplete lineage sorting (i.e., preservation of ancestral polymorphisms; Platt et al., 2019). Methods have been developed to circumvent confounding signals (e.g., ABBA–BABA statistics; Durand et al., 2011; Green et al., 2010) and in principle it is possible to separate introgression from other evolutionary processes (Martin et al., 2014). Research on introgression between divergent species can reveal important contributions to the evolutionary history of the taxa involved (e.g., ecological adaptations; Nelson et al., 2021) and increase our understanding of how such mechanisms can affect contemporary populations in the future and how robust reproductive barriers are against gene flow between divergent species.

There is currently a need for systems to study reproductive isolation in natural populations experimentally (Stankowski & Ravinet, 2021; White et al., 2019). An interesting experimental system for investigating such processes appear in fungal species complexes in the Agaricomycotina. The subphylum Agaricomycotina is a diverse taxon, with about 20 000 species described worldwide and a crown age estimate of around 429 million years (Floudas et al., 2012). Research on hybridization and introgression among species of the Agaricomycotina (mushroom-forming fungi) is limited, but there are some examples from genera including *Pleurotus* (Bresinsky et al., 1987), *Heterobasidion* (Garbelotto et al., 1996; Giordano et al., 2018; Stenlid & Karlsson, 1991) and *Armillaria* (Baumgartner et al., 2012), indicating that hybridization may be a common but understudied mechanism of speciation and gene exchange among taxa in this branch of the tree of life. Moreover, recent research shows that the reproductive barrier in fungi can be permeable despite high divergence between species (Maxwell et al., 2018), making the fungal reproductive system an interesting case study for expanding our knowledge on reproductive isolation and the speciation continuum (Maxwell et al., 2018).

In this study, we use natural populations of *Trichaptum fuscoviolaceum* (Ehrenb.) Ryvarden and *Trichaptum abietinum* (Dicks.) Ryvarden (pictured in Figure 1) as our model organisms. The two species are closely related sister species, forming a monophyletic group in the genus *Trichaptum* (Ko & Jung, 2002; Vlasák & Vlasák, 2017). They are saprotrophic white rot fungi growing on conifers, with a widespread distribution across the boreal realm in the northern hemisphere. The two species are broadly sympatric and can grow on the same host, and sometimes they are found together on the same substrate. They are in general phylogenetically well separated (Kauserud & Schumacher, 2003; Peris et al., 2022; Seierstad et al., 2020), but some individuals clustered incongruently for different loci in a previous study including only a few molecular markers (Seierstad et al., 2020). Here, the authors suggested introgression or incomplete lineage sorting as possible explanations for the conflicting phylogenetic signals (Seierstad et al., 2020). Reproductive barriers between the two species have been documented by in vitro crossing experiments (Macrae, 1967).

Population structure has been found within *T. abietinum* (Peris et al., 2022; Seierstad et al., 2020). In North America, two populations referred to as the North American A and the North American B population occur in sympatry and are reproductively isolated (i.e., form intersterile groups; Macrae, 1967; Magasi, 1976; Peris et al., 2022). Such intersterile groups have not been detected among populations of *T. fuscoviolaceum* (Macrae, 1967; Peris et al., 2022), but some genetic structuring of populations has been observed (Peris et al., 2022; Seierstad et al., 2020).

Through this study, we aimed at exploring how signs of introgression can be discovered in genomes of extant species and how regions retained from the past or current introgression might influence the evolution of contemporary populations. We used the experimental system to investigate potential introgression by conducting whole genome sequencing of individuals belonging to
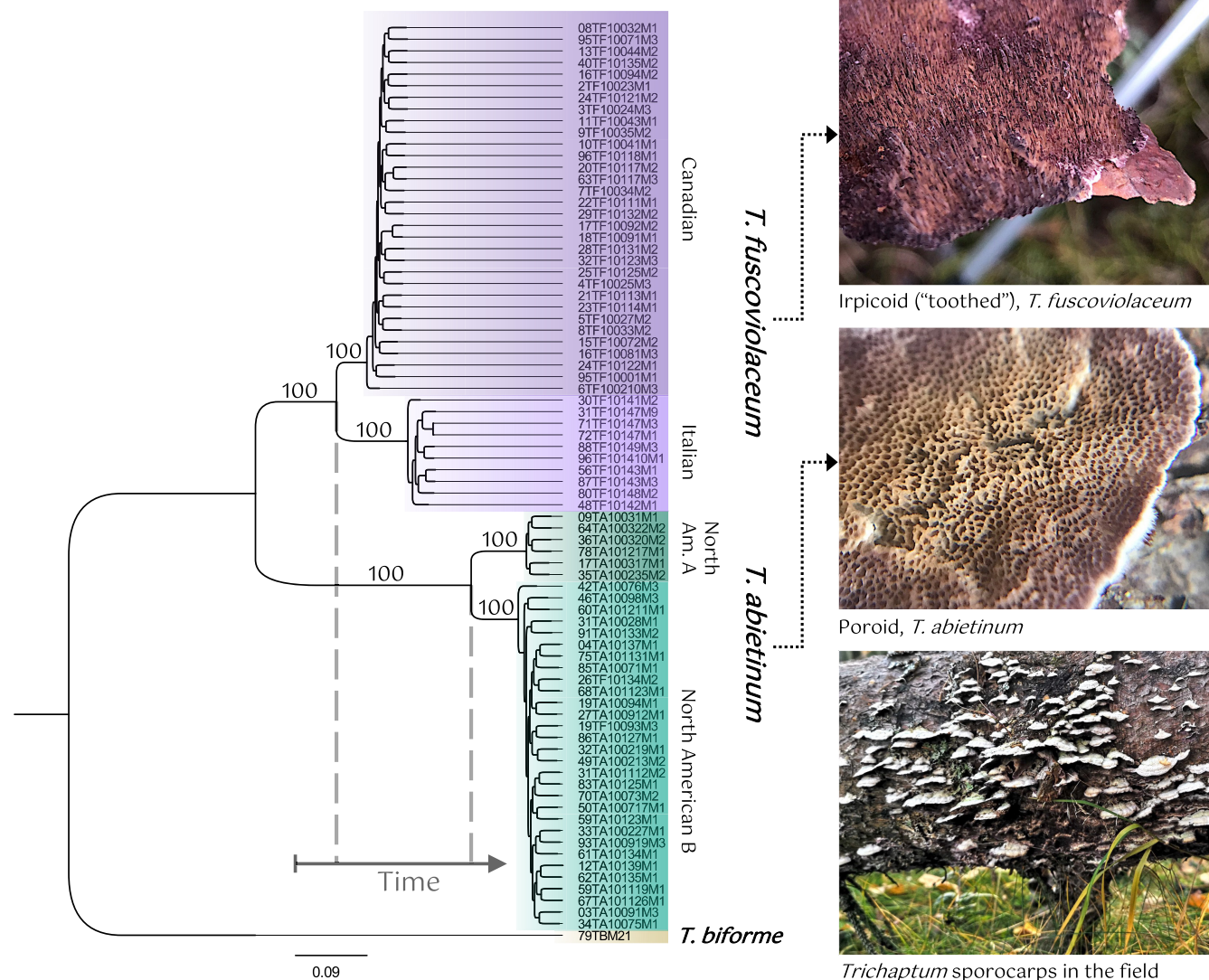
FIGURE 1 Clear population structure in the phylogenetic tree analysis. The analysis is based on a single nucleotide polymorphism (SNP) dataset of 3 118 957 SNPs. The tree is constructed using *IQ-TREE 2* (Minh et al., 2020) with the model GTR+ASC. The numbers on the branches represent bootstrap branch support. Populations of *Trichaptum fuscoviolaceum* (TF) are coloured in shades of purple and populations of *T. abietinum* (TA) are coloured in shades of green. The outgroup, *T. biforme*, is coloured in brown. The scale bar on the bottom is the number of substitutions per site. The time axis illustrates relative split of the TF and TA populations (see Figure S6). The shade of purple of the hymenium (spore producing layer) can vary. The two TF individuals in the North American B population are confirmed as North American B TA individuals after genomic analyses (wrongly assigned in the field). Photographs of hymenia by Inger Skrede and photograph of sporocarps by Malin Stapnes Dahl.

different populations of *T. abietinum* and *T. fuscoviolaceum*. Further, we assessed the possibility of current gene flow by testing compatibility across species through in vitro crossing experiments. We hypothesised that *T. fuscoviolaceum* and *T. abietinum* populations do not hybridize frequently due to a well-resolved phylogeny and earlier crossing experiments revealing the species to be intersterile (Macrae, 1967; Peris et al., 2022; Seierstad et al., 2020). However, due to their overlapping habitat, ecology and morphology, we hypothesised that the sister species might have a shared history that involves introgression, possibly having occurred among ancient populations.

2 | MATERIALS AND METHODS

2.1 | Strains and cultures

Individuals of *T. abietinum* and *T. fuscoviolaceum* from New Brunswick, Canada and individuals of *T. fuscoviolaceum* from Pavia, Italy were included in this study. One individual of *T. biforme* from New Brunswick, Canada, was included as an outgroup. Notes on host substrate, GPS coordinates and locality of all individuals included in this study are presented in Table S1. Single spore cultures and full-genome Illumina sequences were available for all individuals from

the study of Peris et al. (2022). For information about single spore culture preparation, growth conditions, DNA extraction, library preparation and Illumina sequencing, please see Peris et al. (2022).

2.2 | Crossing experiments

To assess mating compatibility, we performed crossing experiments between species (i.e., between individuals of *T. abietinum* and *T. fuscoviolaceum*). As a positive control, we also crossed individuals within *T. fuscoviolaceum*. Some of the crosses between species include European *T. abietinum* for which sequences are included in Peris et al. (2022), but not in the present study. The crossing set-ups were planned according to a mating compatibility scheme based on mating (*MAT*) loci predicted in Peris et al. (2022). We crossed individuals that were both expected and not expected to mate based on their predicted mating type (i.e., dissimilar or similar allelic classes on both *MAT* loci). Individuals (including population assignment) used for the experiment are presented in Table S2 (see Peris et al. (2022) for further details on the European *T. abietinum* individuals). Three replicates were made for all crosses to strengthen the confidence in the observations.

Pairs of monokaryotic individuals (circular 0.8 cm in diameter plugs) were plated 4 cm apart on petri dishes containing 3% MEA. The petri dishes were placed in a dark incubator at 19°C until the two mycelia had grown together (about 2 weeks). The cultures were photographed using a Nikon D600 Digital Camera. To investigate if the crossing experiments were successful, we assessed the presence or absence of clamp connections using a Zeiss Axioplan 2 imaging light microscope with Zeiss AxioCam HRc. Microscopic photographs of hyphae were taken at 400 and 630× magnification.

2.3 | Reference genomes

We used the two genomes of *T. abietinum* (strain TA10106M1) and *T. fuscoviolaceum* (strain TF100210M3) as reference genomes (Bioproject PRJNA679164; https://doi.org/10.5061/dryad.fxpnv x0t4; Peris et al., 2022). Both these strains are collected in New Brunswick, Canada. The *T. abietinum* reference genome strain belongs to the North America B population. In addition, we made a combined reference genome by merging the *T. abietinum* (acc. no. GCA 910574555) and *T. fuscoviolaceum* (acc. no. GCA 910574455) reference genomes with *sppIDer* (Langdon et al., 2018).

2.4 | Preparation and initial mapping of whole genome data

Illumina raw sequences were quality filtered, removing sequences with a Phred quality score less than 30, using *Trim Galore! v0.6.2* (https://www.bioinformatics.babraham.ac.uk/projects/trim_galor e/; Krueger, 2015), and assessed using *FastQC* (Andrews, 2010) and

MultiQC (Ewels et al., 2016). After pre-processing, we used *BWA v0.7.17* (Li & Durbin, 2009) to search for recent hybrids by mapping Illumina reads from *T. fuscoviolaceum* to a combined reference genome of *T. fuscoviolaceum* and *T. abietinum* using the wrapper *sppIDer* (Langdon et al., 2018). The wrapper generates a reference genome with chromosomes from both *T. fuscoviolaceum* and *T. abietinum*. The reads from a strain from one species can then be mapped to the combined genome. If the reads of an individual map equally well to chromosomes of both species, it indicates that the strain is a hybrid. No hybrids were revealed among the *T. fuscoviolaceum* individuals in the *sppIDer* analysis (Figure S1). All *T. fuscoviolaceum* individuals mapped with greater depth to the *T. fuscoviolaceum* part of the combined reference genome than the *T. abietinum* part. Since there were no recent hybrid individuals and we could only use one reference for further analyses, we chose to continue with the *T. fuscoviolaceum* reference genome.

2.5 | Re-mapping with Stampy

To improve mapping of *T. abietinum*, *T. biforme* and the Italian *T. fuscoviolaceum* to the reference genome (based on a Canadian *T. fuscoviolaceum* individual), the raw sequences were mapped with *Stampy v1.0.32* (Lunter & Goodson, 2011), which is designed to be more sensitive to divergent sequences (Lunter & Goodson, 2011), before continuing with further analyses. Based on the nucleotide divergence estimates found in Peris et al. (2022) by conversion of average nucleotide identity using *FastANI* (Jain et al., 2018), the substitution rate flag was set to 0.23 for *T. biforme*, 0.067 for the Italian *T. fuscoviolaceum*, and 0.157 for *T. abietinum* (both the A and B populations) when mapping each to the reference. The raw sequences were not trimmed before mapping due to limitations on hard clipping in *Stampy* (i.e., sequences are sometimes too short for *Stampy*), but poor sequences were filtered away at a later stage (see below).

2.6 | SNP calling and filtering

To obtain a dataset with single nucleotide polymorphisms (SNPs), we first used *GATK HaplotypeCaller v4.1.4* (McKenna et al., 2010). To create the dictionary files and regroup the mapped files before SNP calling, we used *Picard v2.21.1* (https://broadinstitute.github. io/picard/) and reference index files were made using *SAMtools* faidx (Li et al., 2009). We ran *HaplotypeCaller* in haploid mode with otherwise default settings. Subsequently, we used the resulting Variant Call Format (VCF) files in *GATK GenomicsDBImport* (McKenna et al., 2010) to create a database used as input for *GATK GenotypeGVCF* (McKenna et al., 2010), which creates a VCF file containing SNPs for all individuals. *GenomicsDBImport* was used with default settings together with the java options ('--java-options') '-Xmx4g' and '-Xms4g' and an interval text file ('--intervals') containing names of the different scaffolds. *GenotypeGVCF* was used with default settings. To remove indels, bad SNPs and individuals

with high missingness, we filtered the resulting VCF file with *GATK VariantFiltration* (McKenna et al., 2010) and *BCFtools v1.9* filter (Danecek et al., 2021). We used GATK's hard filtering recommendations (https://gatk.broadinstitute.org/hc/en-us/articles/360035890471-Hard-filtering-germline-short-variants) together with the Phred quality score option of removing SNPs with a score less than 30.0 ('QUAL < 30.0'). With *BCFtools* filter, we removed indels and poor SNPs using these options: minimum read depth (DP) < 3, genotype quality (GP) < 3 and '-v snps'. We also used *BCFtools* filter to remove multiallelic SNPs ('view -M2'), SNPs close to indels ('--SnpGap 10'), variants with a high number of missing genotypes ('-e "F_MISSING > 0.2"'), minimum allele frequency ('MAF <= 0.05'), and invariant sites and monomorphic SNPs ('-e "AC==0 || AC==AN"'). We made one dataset where monomorphic SNPs were removed and the MAF filter was applied (Dataset 1 with 2 040 885 SNPs) and two datasets, one with the outgroup and one without, not applying these filters (Dataset 2 with 3 065 109 SNPs; Dataset-O 2 with 3 118 957 SNPs, where O = outgroup), because monomorphic sites were required to calculate some divergence statistics. After filtering, individuals with high missingness or high heterozygosity (i.e., dikaryons) were removed. The final datasets consisted of 32 individuals from the Canadian *T. fuscoviolaceum* population, 9 individuals from the Italian *T. fuscoviolaceum* population, 30 individuals from the North American B *T. abietinum* population, and 6 individuals from the North American A *T. abietinum* population (https://doi.org/10.5061/dryad.xpnvx0kkz).

2.7 | Phylogenetic tree analysis

To confirm the phylogenetic relationship between the different populations of *T. abietinum* and *T. fuscoviolaceum*, we performed a maximum likelihood phylogenetic tree analysis using *IQ-TREE 2* (Minh et al., 2020). The analysis was run with the standard general time reversible (GTR) substitution model and ascertainment bias correction (ASC) to account for the fact that only variable sites were used. The VCF-file from Dataset-O 2 was converted into a PHYLIP file by using Edgardo M. Ortiz's script vcf2phylippy. The IQ-TREE analysis was run on the PHYLIP file using the flags '-T auto', '-m GTR+ASC', '-alrt 1000' and '-B 1000'.

2.8 | Principal component and divergence analyses

To explore the data and investigate population groupings, we performed a principal component analysis (PCA) with *PLINK v2.00-alpha* (www.cog-genomics.org/plink/2.0/; Chang et al., 2015). To prepare the input file, we linkage pruned Dataset 1 in *PLINK*, using the flags '--vcf $vcf_file', '--double-id', '--allow-extra-chr', '--set-missing-var-ids @:#', '--out $out_file' and '--indep-pairwise 50 10 0.1', retaining 56 046 SNPs. The '--indep-pairwise' flag performs the linkage pruning, where '50' denotes a 50 Kb window, '10' sets the window step size to 10 bp, and '0.1' denotes the r^2

(or linkage) threshold. A PCA was subsequently performed on the pruned VCF file, using the flags, '--vcf $vcf_file', '--double-id', '--allow-extra-chr', '--set-missing-var-ids @:#', '--extract $prune.in_file', '--make-bed', '--pca', and '--out $out_file' (both linkage pruning and PCA flags were based on the Physalia tutorial https://speciationgenomics.github.io/pca/).

To investigate the divergence between populations, we applied a sliding window approach on Dataset 2 to calculate the fixation index (F_{ST}) and the absolute divergence (d_{XY}) along the genome. We also performed a sliding window analysis to calculate within population divergence (π). The analyses were performed using the Simon Martin's script popgenWindowspy with *Python v3.8* (Van Rossum & Drake, 2009). We set the window size to 20 000 bp ('-w 20000'), step to 10 000 bp ('-s 10000') and the minimum number of SNPs in each window to 10 ('-m 10').

2.9 | Introgression analyses with D-statistics

To investigate introgression between populations, we used the *R* (R Core Team, 2020) package *admixr* (Petr et al., 2019) and Dataset-O 2 to calculate the *D* (Durand et al., 2011; Green et al., 2010), outgroup f_3 (Raghavan et al., 2014) and f_4-ratio (Patterson et al., 2012; Reich et al., 2009, 2011) statistics between different populations (based on recommendations from the Physalia tutorial https://speciationgenomics.github.io/ADMIXTOOLS_admixr/, and the *admixr* tutorial https://bodkan.net/admixr/articles/tutorial.html#f4-ratio-statistic-1). To prepare the input file from VCF to Eigenstrat format, we used the conversion script convertVCFtoEigenstrat.sh CIDEGENT/2021/039), which utilizes *VCFtools v0.1.16* (Danecek et al., 2011) and *EIGENSOFT v7.2.1* (Patterson et al., 2006; Price et al., 2006). The script has a default recombination rate of 2.0 cM/Mb, which we changed to 2.5 cM/Mb based on earlier findings in the class Agaricomycetes, where *Trichaptum* belongs (Heinzelmann et al., 2020).

We further used another *Python* script developed by Simon Martin, ABBABABAwindowspy, for a sliding window ABBA–BABA analysis on Dataset-O 2 to calculate the proportion of introgression (f_{dM}; Malinsky et al., 2015). The window size was set to 20 000 ('-w 20000'), step size to zero, and minimum number of SNPs per window to 100 ('-m 100'), together with '--minData 0.5' to specify that at least 50% of the individuals in each population must have data for a site to be included (based on recommendations from the Physalia tutorial https://speciationgenomics.github.io/sliding_windows/). We used *T. biforme* as outgroup and tested introgression between the Canadian *T. fuscoviolaceum* and the *T. abietinum* populations in addition to the Italian *T. fuscoviolaceum* and the *T. abietinum* populations (the phylogenetic topology was based on results from the f_3 analysis). Outlier windows were extracted from the results with a Hidden Markov-model approach using the *R* package *HiddenMarkov* (Harte, 2021) following Ravinet et al. (2018). Briefly, windows were classified as either a peak or non-peak state by comparing them to a null distribution derived

from chromosome-specific permutation tests. These were obtained by randomly shuffling nucleotide sequences and then performing analyses with sliding window sizes from 5 to 10 kb. Transition probabilities between valleys and non-valleys were symmetrical, with an emphasis on it being difficult to transition between states ($p = 0.1$), but easy to remain within states ($p = 0.9$) (Ravinet et al., 2018). Since the HMM approach cannot analyse negative values, the f_{dM} distribution was rescaled by adding 2 to all values. Annotated genes in these outlier windows were retrieved from the annotated *T. fuscoviolaceum* reference genome. The reference genome was annotated using *RepeatModeler* (Flynn et al., 2020), *RepeatMasker* (Smit et al., 2013–2015) and *MAKER2* (Holt & Yandell, 2011). Functional annotation and protein domain annotations of detected coding sequences and the encoded proteins were performed using *blastp* (Altschul et al., 1990) against a local UniProt database and InterProScan (Jones et al., 2014), respectively. All the annotations were encoded in a General Feature Format (GFF) file, which was used to match the significant windows and extract the genes. Gene ontology terms annotated in the GFF file were extracted using the package *rtracklayer v1.48* (Lawrence et al., 2009) in *R*. Gene ontology (GO) enrichment analysis was performed in *R* using the *TopGO v2.40* package (Alexa & Rahnenfuhrer, 2021). Lastly, a false discovery rate (FDR) analysis was performed on the resulting raw *p*-values.

2.10 | Network analysis with TreeMix

To further explore possible introgression events and direction of introgression, we applied a network analysis with *TreeMix* (Pickrell & Pritchard, 2012). To prepare the VCF-file (Dataset-O 2) for analysis, we removed sites with missing data using *VCFtools* (with '--max-missing 1') and linkage pruned the data using *PLINK*. Linkage pruning was performed in the same way as with the PCA, except the file was recoded into a new VCF file using the flags '--bfile' and '--recode vcf' after pruning. To convert the data to *TreeMix* format, we ran Joana Meier's script vcf2treemixsh. The script *vcf2treemix.sh* also requires the script plink2treemixpy.

TreeMix was run using the options '-global' and '-root *T_biforme*'. The option for number of edges ('-m') was analysed from 1 to 10 and the option for block size ('-k') was varied between 300–800 with 100 between each block size. The variation in block size is included to avoid convergence on identical likelihoods for replicate runs, which tends to happen when the signal in the data is strong (Fitak, 2021). These likelihoods are used to calculate a standard error for the downstream evaluation of the output with *OptM* (Fitak, 2021), but the standard error cannot be calculated in cases where the replicate runs have identical likelihoods. For each block size, the analysis was repeated three times for 'm' 1–10 edges. To find the optimal number of edges, we ran *OptM* in *R*. The residuals and network with different edges were plotted in *R* using the functions provided by *TreeMix* (*plotting_funcs.R*) together with the packages *RColorBrewer v1.1–2* (Neuwirth, 2014) and *R.utils* (Bengtsson, 2021).

2.11 | Demographic modelling

To explore divergence and introgression, we applied demographic modelling with *fastsimcoal2* (Excoffier et al., 2021). Fastsimcoal2 uses coalescent simulations under a given demographic model to generate site frequency spectra, and by comparing these to the observed site frequency spectrum in the data, it is possible to identify the most likely demographic scenario among the specified models. The program also allows for parameter estimation. To prepare the data (Dataset 2) for analysis, site frequency spectrum files were created using *easySFS* (https://github.com/isaacovercast/easySFS). Subsequently, *fastsimcoal2* was run using the output files from *easySFS* together with a template file defining the demographic model and a parameter estimation file (scripts and example files are archived at https://zenodo.org/badge/latestdoi/619255024). The analyses were run with the flags '-m', '-0', '-n 200000', '-L 50', '-s 0' and '-M', which specifies 50 cycles of 200000 coalescent simulations per cycle, and to only consider polymorphic sites in the site frequency spectra (i.e., ignore monomorphic sites). The mutation rate was set to 1e-7. Each model was run 100 times and the run with the best likelihood was extracted using Joana Meier's script fscselectbestrunsh. We selected several different models based on likely events inferred from the results of the ML tree, *D* and *f* statistics, and *TreeMix* analyses to test for different scenarios of introgression, both with and without one or two ghost populations (Figure S7). To compare different models, an AIC value was calculated from the run with the best likelihood for each model using the *R* script based on code by Vitor Sousa, calculateAICsh. Since AIC can overestimate support for the best model when SNPs are in linkage, we also calculated the likelihood distributions using the best run from all the models. The models were run with the best parameter values ({PREFIX}_maxL. par output from the first run) 100 times in *fastimcoal2* with the options '-n 1000000', '-m', '-q', and '-0', which specifies 1000000 simulations and to only consider polymorphic sites. The likelihood values were collected and plotted in *R* for comparison between models (i.e., look for overlapping distributions).

3 | RESULTS

3.1 | Crossing experiments confirm incompatibility between species

To ensure that the previous results of intersterility between *T. abietinum* and *T. fuscoviolaceum* were also the case for our collections, we performed crossing experiments with our individuals. We did not observe clamp connections between crosses of *T. fuscoviolaceum* and *T. abietinum* individuals. This was the case both for mate pairs that were predicted to mate based on mating type alleles and for those predicted not to (Table S2; Figures S2 and S4; mating type alleles were annotated in Peris et al., 2022). It was difficult to observe compatible crosses by investigating the cultures macroscopically, but there was often a sharper line between individuals on the petri

dish when the crosses were incompatible (Figure S2). The *T. fuscovio-laceum* individuals mated as expected within species (i.e., those that were predicted to be incompatible due to identical mating types showed no clamp connections and those that were predicted to be compatible had clamp connections; Table S2; Figures S3 and S5).

3.2 | Phylogeny, principal component and divergence analyses reveal highdivergence between species

The maximum likelihood (ML) phylogeny clustered the species and populations into well-defined clades with high support (Figure 1).

The PCA also indicated clear groupings of species and popula-tions of *T. fuscoviolaceum* and *T. abietinum*, with PC1 and PC2 ex-plaining 57.5% and 12.2% of the observed variation, respectively (Figure 2). Population clusters are concordant with the groups in the phylogenetic tree analysis.

The clear distinction spotted in the PCA was corroborated by the fixation index (F_{ST}), which showed a high degree of divergence both between populations of different species and between populations of same species. The F_{ST} means across the genome for between species comparisons were ranging from 0.6 to 0.8 (Table 1). The within-species comparisons showed higher differentiation between the two *T. fuscoviolaceum* populations than between the *T. abietinum* populations (Table 1).

The absolute between populations divergence (d_{XY}) echoed the patterns of the PCA and F_{ST} scan, with generally high divergence both between populations of different species and between pop-ulations within species. The mean d_{XY} values between populations of different species were about 0.4, while the mean values between populations of same species were slightly less than 0.2 for both com-parisons (Table 1).

The within population variation calculated by the nucleotide di-versity, π, had a mean value of about 0.05 for all populations (Table 1).

3.3 | Introgression analyses indicate a complex evolutionary history

The divergence analyses suggested that the species had diverged for a long time. Thus, we wanted to explore signs of ancestral introgres-sion not revealed by assessing current interbreeding with crossing experiments. The *D* statistic, used to detect signs of introgression across the genome, gave significant *D* values (|z-score| > 3) between the Italian *T. fuscoviolaceum* and both of the *T. abietinum* populations (Table 2), indicating introgression between the Italian *T. fuscovio-laceum* and the *T. abietinum* populations. The test of introgression between the *T. abietinum* populations and either of the *T. fuscovio-laceum* populations did not reveal significant positive or negative *D* values. There was also a larger discrepancy between ABBA and BABA sites in the significant topologies (Table 2, row three and four), than in the nonsignificant topologies (Table 2, row one and two).

The four-population *f* statistic (f_4 ratio), used to test proportion of introgression, resulted in a violation of the statistical model (i.e., negative alpha values; valid values are proportions between 0 and 1) when placing *T. abietinum* and *T. fuscoviolaceum* as sister groups with the Canadian *T. fuscoviolaceum* or the North American B *T. abietinum* at the X position (Table 3). Reversing the positions of the Canadian and Italian *T. fuscoviolaceum* or the two *T. abietinum* populations at X and C resulted in a positive alpha value, which did not violate the model (Table 3). The alpha value indicated about 5.7% shared ancestry between the *T. abietinum* populations and the Italian *T. fuscoviolaceum* population (Table 3, row three and four). The small amount of shared ancestry (0.1%–0.2%) between the North American A *T. abietinum* and the two *T. fuscoviolaceum* populations did not show a significant *z*-score (<3; Table 3, rows seven and eight).

Further investigation of introgression with the three-population outgroup *f* statistic (f_3), which estimates shared genetic drift (or branch length), revealed that the *T. abietinum* populations split later (share more genetic drift) than the *T. fuscoviolaceum* populations (Figure S6; Figure 1). As with the f_4 ratio analysis, the Italian *T. fuscoviolaceum*

FIGURE 2 Clear groupings according to species and populations in the principal component analysis (PCA). The PCA is based on a single nucleotide polymorphism (SNP) dataset of 2 040 885 SNPs linkage pruned to 56 046 SNPs. The *x*- and *y*-axes represent PC1 and PC2, respectively, with percentage of variance explained in parentheses. Points are individuals coloured by population as indicated in the legend. TA, *Trichaptum abietinum*; TF, *Trichaptum fuscoviolaceum*. The figure is made in *R v4.0.2* using the packages *ggplot2* (Wickham, 2016) and *wesanderson* (Ram & Wickham, 2018).
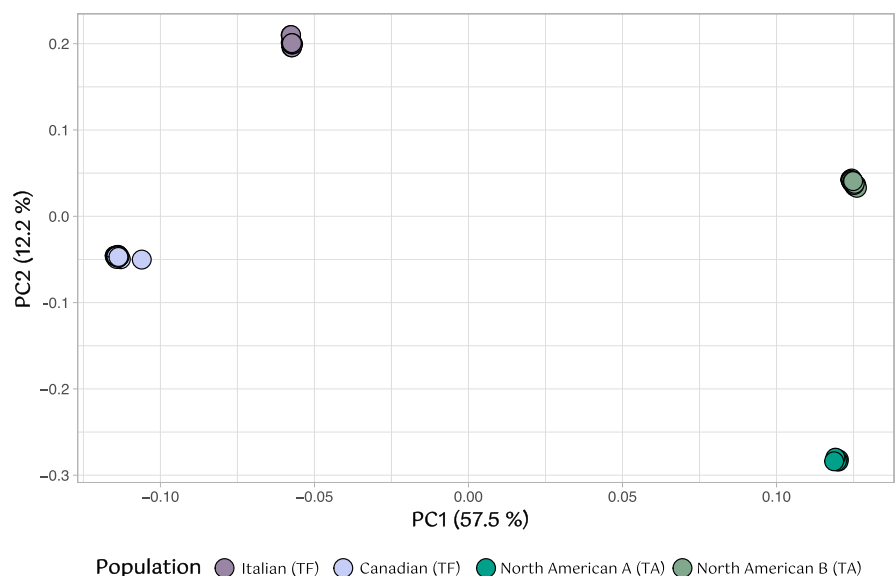
TABLE 1 F_{ST} and d_{XY} show high degree of divergence.

DIVERGENCE STATISTICS		
Population comparisons	F_{ST} (mean)	d_{XY} (mean)
North American A TA vs. Canadian TF	0.61	0.39
North American A TA vs. Italian TF	0.77	0.42
North American B TA vs. Canadian TF	0.72	0.39
North American B TA vs. Italian TF	0.67	0.42
Canadian TF vs. Italian TF	0.46	0.17
North Americ A TA vs. North American B TA	0.33	0.16
NUCLEOTIDE DIVERSITY		
Populations		π (mean)
Canadian TF		0.056
Italian TF		0.046
North American A TA		0.057
North American B TA		0.060

Note: The analyses are performed on a single nucleotide polymorphism (SNP) dataset of 3 065 109 SNPs. The analyses were run as sliding windows and only the mean estimates across the genomes are presented here. The table includes which populations the divergence statistics are calculated between (population comparisons), the mean fixation index (F_{ST}) and the mean absolute divergence between populations (d_{XY}). Below, the mean within population nucleotide diversity (π) is displayed.

Abbreviations: TA, *Trichaptum abietinum*; TF, *Trichaptum fuscoviolaceum*.

TABLE 2 The *D* statistic indicates introgression.

D STATISTICS									
W	X	Y	Z	*D*	Std error	*z*score	BABA	ABBA	*n* SNPs
NamB TA	NamA TA	Can TF	TB	−0.0041	0.004744	−0.868	9142	9217	662 894
NamA TA	NamB TA	It TF	TB	0.0060	0.005929	1.018	9706	9590	662 712
Can TF	It TF	NamA TA	TB	−0.2257	0.008558	−26.376	8072	12 776	662 712
It TF	Can TF	NamB TA	TB	0.2287	0.009069	25.221	12 810	8041	664 963

Note: The analysis is performed on a single nucleotide polymorphism (SNP) dataset of 3 118 957 SNPs. The *D* statistic is based on a phylogenetic tree hypothesis of (((W, X), Y), Z) and tests introgression between Y and X (negative D) and Y and W (positive D). Z is the outgroup. The table includes the *D* value (*D*), standard error (std error), significance of the *D* values (z-score; an absolute z-score larger than 3 is considered significant), the number of SNPs shared between Y and W (BABA), the number of SNPs shared between Y and X (ABBA), and the number of SNPs used for the comparison (*n* SNPs).

Abbreviations: Can TF, Canadian *Trichaptum fuscoviolaceum*; It TF, Italian *Trichaptum fuscoviolaceum*; NamA TA, North American A *Trichaptum abietinum*; NamB TA, North American B *Trichaptum abietinum*; TB, *Trichaptum biforme*.

population exhibited slightly more shared genetic drift with the *T. abietinum* populations than the Canadian *T. fuscoviolaceum* population. Nevertheless, the difference between the two *T. fuscoviolaceum* populations was miniscule. The f_3 analysis indicated a phylogenetic topology where the *T. fuscoviolaceum* populations diverged earlier than the *T. abietinum* populations. A reasonable next step was, therefore, to test introgression between the *T. abietinum* populations and each of the *T. fuscoviolaceum* populations in subsequent sliding window introgression analyses (i.e., a (((North American B *T. abietinum*, North American A *T. abietinum*), *T. fuscoviolaceum* population), *T. biforme*) phylogenetic topology; see below).

The network analysis conducted in *TreeMix*, based on the model with the most optimal number of edges, supported introgression from the Italian *T. fuscoviolaceum* into the North American B *T. abietinum* population (Figure 3). From the residual plot (Figure S8, 1 edge), it was clear that a large proportion of the residuals were not accounted for between the Italian *T. fuscoviolaceum* and the North American B *T. abietinum*. When testing which number of edges was the most optimal, the model with 1 migration edge got the best support (Figure S9).

The sliding window proportion of introgression (f_{dM}) calculated across the genome, which was set up based on the results from the f_3 analysis, revealed small regions of possible introgression (Figure 4; Figure S10). There were several windows of significant positive f_{dM} values (e.g., more shared derived polymorphisms than expected between the *T. fuscoviolaceum* populations and the North American A *T. abietinum* population), which suggests regions of introgressed genes (HMM outliers are marked in Figure 4 and Figure S10, and

TABLE 3 The four-population f statistic (f_4) show further signs of introgression.

F_4 RATIO							
A	B	X	C	O	Alpha	Std error	**z**score
NamA TA	NamB TA	Can TF	It TF	*T. biforme*	−0.061072	0.003619	−16.878
NamB TA	NamA TA	Can TF	It TF	*T. biforme*	−0.060432	0.003553	−17.010
NamB TA	NamA TA	It TF	Can TF	*T. biforme*	0.057001	0.003160	18.038
NamA TA	NamB TA	It TF	Can TF	*T. biforme*	0.057569	0.003215	17.906
It TF	Can TF	NamB TA	NamA TA	*T. biforme*	−0.002591	0.002536	−1.022
Can TF	It TF	NamB TA	NamA TA	*T. biforme*	−0.001535	0.001703	−0.902
Can TF	It TF	NamA TA	NamB TA	*T. biforme*	0.001536	0.001697	0.905
It TF	Can TF	NamA TA	NamB TA	*T. biforme*	0.002592	0.002522	1.028

Note: The analysis is based on a single nucleotide polymorphism (SNP) dataset of 3 118 957 SNPs. The table shows the different configurations tested from a hypothesis of the phylogenetic relationship presented as (((A, B), (X, C)), O), where X is the introgressed population and C its sister population, with the B population as the source of introgression and A as its sister population. O is the outgroup (*Trichaptum biforme*). The alpha value indicates proportion of gene flow with standard error (std error) and significance (*z*-score; considered significant when larger than 3). Negative alpha values are due to violation of the statistical model.

Abbreviations: Can, Canadian; It, Italian; NamA, North American A; NamB, North American B; TA, *T. abietinum*; TF, *T. fuscoviolaceum*.

FIGURE 3 Introgression from the Italian *Trichaptum fuscoviolaceum* into the North American B *T. abietinum*. The plot is based on results from the *TreeMix* (Fitak, 2021) analysis with a block size (-k) of 700 and 1 migration edge (-m 1). The yellow arrow shows the direction of migration (introgression). The bar on the left depicts the migration weight (proportion of admixture). The bottom scale bar shows the drift parameter (amount of genetic drift along each population; Wang et al., 2016). TF, *T. fuscoviolaceum*; TA, *T. abietinum*; The outgroup is *T. biforme*.
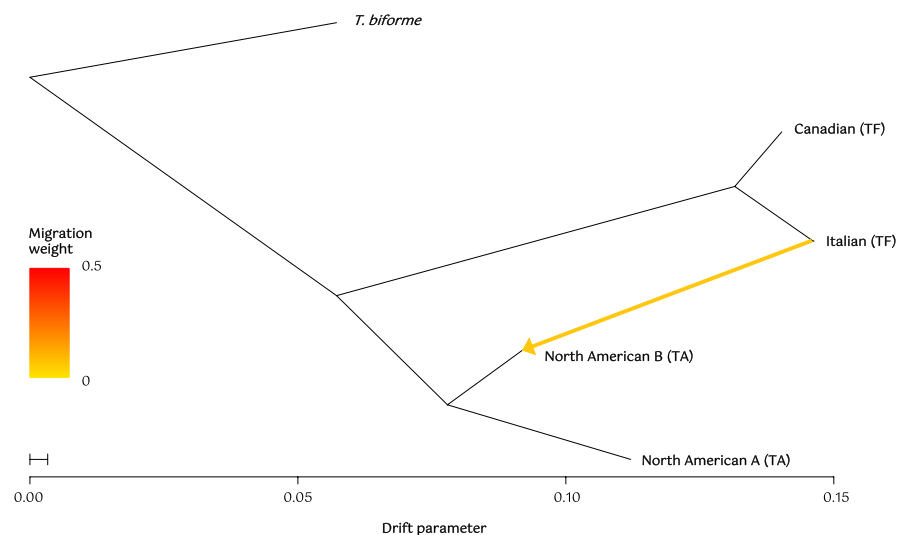
presented in Table S3). The genes in outlier windows coded for many unknown proteins, but also proteins similar to those found in common model organisms such as *Saccharomyces* spp. and *Arabidopsis thaliana*. The genes with similarity to other organisms are annotated to many different functions (i.e., there are genes involved in oxidoreductases, hydrolases, and transport, among others; The UniProt Consortium, 2021). The GO enrichment analysis found some of the HMM outlier genes to be involved in metabolic processes and copper ion transport, to name a few (Table S4). However, after running FDR analysis on the raw p-values, none of the enrichment terms were significant.

3.4 | Demographic modelling indicates involvement of a ghost population

Lastly, we conducted demographic modelling to gain insight into divergence times and introgression events. We were also able to include a ghost population (Beerli, 2004) to test for introgression from unsampled or extinct populations. The best model, supported by both AIC and likelihood distribution comparison, showed introgression occurring twice; first between an ancestral *T. fuscoviolaceum* population and an ancestral *T. abietinum* population and later between a more recent ghost population related to the Italian *T. fuscoviolaceum* and the North American B *T. abietinum* (Figure 5; Figure S7, Ghost migration 9; Figure S11). These results were partly congruent with the network analysis where introgression was inferred between the Italian *T. fuscoviolaceum* and the North American B *T. abietinum* (Figure 3), but in the network analysis a ghost population could not be included. The best supported model further indicated that the sister species split 524 473 generations ago, while the *T. fuscoviolaceum* populations split 99 101 generations ago and the *T. abietinum* populations 92 260 generations ago. The estimated split of the ghost population from the Italian *T. fuscoviolaceum* populations was 94 536 generations ago (Figure 5; Table S5). The analysis also showed that there were few
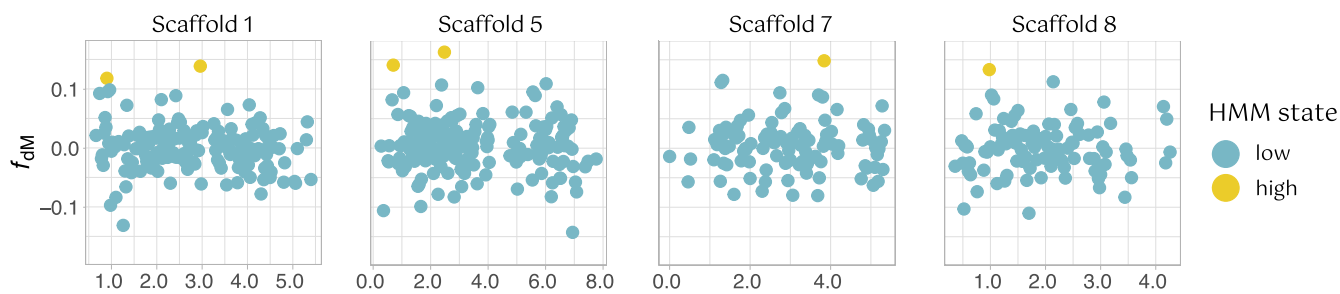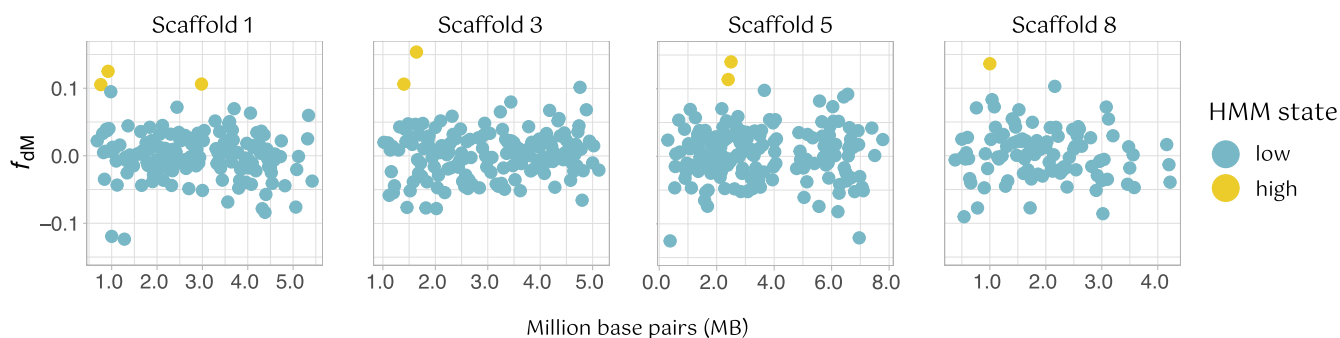
FIGURE 4 Signs of scattered introgression throughout the genome. A proportion of introgression (f_{dM}) sliding window analysis based on a single nucleotide polymorphism (SNP) dataset of 3 118 957 SNPs, where windows with at least 100 SNPs are included. Only four of the scaffolds are depicted here for each of the analyses. The remaining scaffolds are shown in Figure S10. The main headers depict the phylogenetic hypothesis, (((P1, P2), P3), O), where P1, P2 and P3 are populations investigated for introgression and O is the outgroup. A positive value indicates more shared derived polymorphisms than expected between P2 and P3, while a negative value indicates the same for P1 and P3. Each point is the f_{dM} value of a window (window size = 20 000 base pairs). Y-axes show the f_{dM} value and x-axes represent million base pair (Mb) position of the windows on the scaffolds. The legend shows the Hidden Markov-model (HMM) state of the windows. Blue coloured points (low) indicate insignificant amount of introgression, while yellow-coloured points (high) are outlier windows with significant introgression from the HMM analysis. Annotated genes in the outlier windows can be found in Table S3. TA, *Trichaptum abietinum*; TF, *Trichaptum fuscoviolaceum*. The figure is made in *R v4.0.2* using the packages *tidyverse* (Wickham et al., 2019) and *wesanderson* (Ram & Wickham, 2018).

migrants between the ancestral populations and a little more between the ghost population and the North American B *T. abietinum* population, but mostly from the ghost population into the North American B (migration values; Figure 5).

4 | DISCUSSION

4.1 | Divergent sister species show signs of introgression

Population genomic and introgression analyses present a window into exploring the dynamics of populations, their genomes and how they evolve. By searching beyond current phylogenies and population structures, intricate evolutionary histories can be revealed. Our study presents several results indicating that high divergence between *T. abietinum* and *T. fuscoviolaceum* does not exclude the possibility of admixture.

Firstly, highdivergence values are prevalent throughout the genomes. The large genetic differences between the species can be a result of mechanisms such as reproductive isolation (Nei et al., 1983) and random events over time (i.e., genetic drift; Watterson, 1985). The fungi make up an ancient and diverse kingdom that originated over a billion years ago (Berbee et al., 2020), with the oldest fungal-like fossil dating back to 2.4 billion years ago (Bengtson et al., 2017) and an estimate of 2–5 million extant species (Li et al., 2021). The divergence of the order Hymenochaetales, which *Trichaptum* belongs to, dates to the Jurassic, about 167 million years ago (Varga et al., 2019). There are 37 accepted species in the genus (Index Fungorum, 2021), but no estimates of the age of *Trichaptum*. Seeing the old age of Hymenochaetales and assuming the genus *Trichaptum* is old, time is a likely explanation for the genome wide high divergence between *T. fuscoviolaceum* and *T. abietinum*. The demographic modelling also suggests that the two species split quite some time ago (524 473 generations).
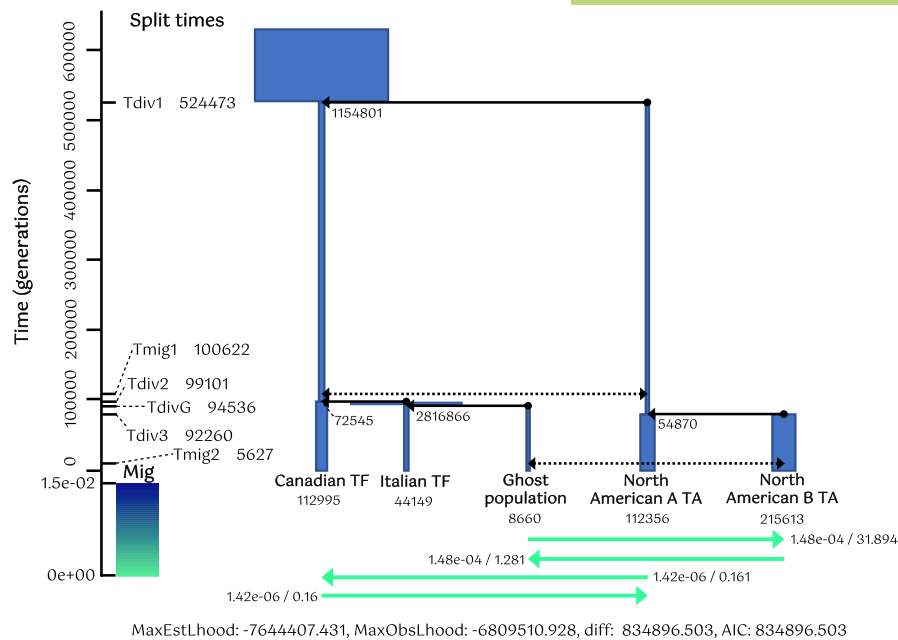
FIGURE 5 Demographic modelling indicates both ancient introgression and introgression from a recent ghost population. The analysis is performed in *fastsimcoal2* (Excoffier et al., 2021) using a dataset of 3 065 109 SNPs. The figure shows the best supported model. The left side of the axis indicate time in generations, with the lower part (below 0; colour bar) showing proportion of migration. The split times (divergence times) and migration times are presented on the right side of the axis. The blue bars and fully drawn black arrows show the estimated effective population sizes and splits, respectively. Effective population sizes are also written next to the splits and below the current populations. The dotted black arrows are the introgression events. The green arrows display the amount of migration (related to the colour bar) with the proportion of introgression estimate/conversion to the number from the effective population size (current populations) that migrated. diff., difference between MaxEstLhood and MaxObsLhood; MaxEstLhood, maximum estimated likelihood; MaxObsLhood, maximum observed likelihood; mig, migration; TA, *Trichaptum abietinum*; Tdiv, time of divergence; TF, *Trichaptum fuscoviolaceum*; Tmig, time of migration. Note: All the parameters (including migration) are plotted backward in time and in haploid numbers.

Today, the sister species occur in the same habitat, with similar morphology and ecology, acting as early saprotrophs on newly deceased conifers in the northern hemisphere (Kauserud & Schumacher, 2003). As mentioned, the two species can grow on the same host and are sometimes found on exactly the same substrate. However, *T. fuscoviolaceum* is usually found on pine (*Pinus*) and fir (*Abies*; most individuals in this study were collected on balsam fir; *A. balsamea*), while *T. abietinum* is more common on spruce (*Picea*) and larch (*Larix*; Macrae, 1967; Peris et al., 2022). Even though habitats overlap, the crossing experiments corroborate previous results (Macrae, 1967) in that the sister species do not hybridize in vitro, and the genomic analyses suggest that this does not happen often between contemporary populations in the wild either. However, the detection of gene flow between more recent populations in the demographic modelling does imply that mating between species can occur occasionally in nature.

The crossing experiments between *T. fuscoviolaceum* individuals of different populations demonstrate that individuals can still mate successfully even though the divergence analyses exhibit high F_{ST} and d_{XY} values. The high divergence could be due to geographic separation of the Italian and Canadian populations, reducing gene flow between these populations. Compatibility is not observed among all populations of *T. abietinum*, where intersterility is detected between some populations that occur in sympatry (Macrae, 1967; Magasi, 1976).

The genus *Trichaptum* consists of tetrapolar fungi, which means individuals are compatible only when they have different alleles on both of the two mating loci (*MATA* and *MATB*; Fraser et al., 2007; Peris et al., 2022). Previous studies have shown that fungal mating loci are diverse and maintained by balancing selection (James et al., 2004; May et al., 1999), which was recently demonstrated in *Trichaptum* as well (Peris et al., 2022). Among species of *Trichaptum*, and within *T. abietinum*, additional reproductive barriers other than incompatible mating loci are at play, causing intersterility. However, such barriers can remain incomplete. If reproductive barriers were incomplete during the divergence of *T. abietinum* and *T. fuscoviolaceum*, and they diverged mostly due to genetic drift in geographic isolation, conserved diversity on the mating loci (as observed in Peris et al., 2022) over time can have allowed for introgression by maintaining reproductive compatibility across species. The demographic modelling does suggest that introgression happened quite some time after the split between the species. This again supports allopatric divergence, making it possible for the species to reproduce at a later stage due to the possible lack of reproductive barriers (no reinforcement). Gene flow between divergent species of fungi has been detected before (e.g., Maxwell et al., 2018). This could be facilitated by the flexible developmental biology of some fungi, with the capability of tolerating developmental imprecision and distortion of their genetic makeup and still be able to grow and reproduce (Moore et al., 2011; Stukenbrock, 2016).

The specific mechanisms behind how the two species diverged are difficult to untangle based on our results. However, the *D* and *f* statistics, together with the network analysis and demographic modelling, show signs of introgression between *T. abietinum* and *T. fuscoviolaceum*. Based on the *D* statistic, the ancestor of the Italian *T. fuscoviolaceum* population appears to have admixed with the *T. abietinum* populations. This might be somewhat counter-intuitive, as it is the Canadian *T. fuscoviolaceum* population that currently occurs in sympatry with the collected *T. abietinum* populations. However, reproductive barriers can be produced between species in sympatry due to reinforcement (Abbott et al., 2013). When an allopatric lineage, such as the Italian *T. fuscoviolaceum* or a closely related ghost population, is encountered, reproductive barriers may not be in place and gene flow can occur. The f_4 ratio test further corroborates these results, indicating that the Italian *T. fuscoviolaceum* shares a larger proportion of the genome with the *T. abietinum* populations than the Canadian *T. fuscoviolaceum*. The violation of the statistical model for some topologies with *T. abietinum* and *T. fuscoviolaceum* populations as sister species in the f_4 ratio test can be due to lack of data from populations not sampled (extinct and extant; i.e., ghost populations; Beerli, 2004), suggesting a more complex evolutionary history of *Trichaptum* than the collected data can disclose. This is corroborated by the demographic modelling, where the best model includes introgression between a ghost population related to the Italian *T. fuscoviolaceum* and the North American B *T. abietinum* population. According to the network analysis, introgression has occurred from the Italian *T. fuscoviolaceum* population into the North American B *T. abietinum* population. However, *TreeMix* is not always able to reveal the true introgression scenario when the actual admixed populations are related to the populations used in the analyses (Fitak, 2021). Therefore, introgression has not necessarily occurred between these two populations but most likely between the ghost population incorporated in the demographic modelling and the North American B *T. abietinum* population. This is similar to introgression inferred between archaic hominins, such as Denisovans and Neanderthals, and present-day humans (Durvasula & Sankararaman, 2019). A wider collection, including more populations across the northern hemisphere (e.g., Asia and throughout Europe and North America), could possibly capture the ghost population (if extant) and help untangle the shared evolutionary history of *T. abietinum* and *T. fuscoviolaceum*. Further, a larger sample could also be used to generate hypotheses of plausible geological or glaciological events leading to the split of these two species.

The f_{dM} analysis shows only slightly more significantly introgressed regions between the Italian *T. fuscoviolaceum* population tested against the *T. abietinum* populations than the Canadian *T. fuscoviolaceum* (14 vs. 11). All the introgressed regions occur between the *T. fuscoviolaceum* populations and the North American A population (not including B as in the other analyses). The demographic modelling did detect introgression between an ancestral *T. fuscoviolaceum* population and a *T. abietinum* population leading up to the current North American A population. Since this event is

ancient, introgressed genes have had time to spread and become fixed in the genomes of current populations (in this case the North American A population and the *T. fuscoviolaceum* populations), which could explain why significant regions are only detected between the North American A population and the *T. fuscoviolaceum* populations.

Many of the genes are also found in the same regions across the genome for both comparisons. This further suggests that the f_{dM} analysis is detecting ancestral and not recent gene flow because the regions are conserved through the population splits (i.e., the introgression happened before the current populations diverged). The small regions of scattered introgression in the f_{dM} analysis also imply more ancient introgression. This follows similar patterns with highly divergent genomes and localized regions of introgression as found in analyses of three-spined stickleback species pairs in the Japanese archipelago (Ravinet et al., 2018) and *Heliconius* butterflies in Brazil (Zhang et al., 2016).

4.2 | Population histories, introgression and its implications

In this study, we only have four populations of two widespread species, thus we are not covering the full diversity of the species. Still, the analyses are able to detect intricate population histories including both a population that is not sampled and ancestral populations leading up to the current ones (i.e., ghost populations). The chance of being able to sample all populations or have no ghost populations in an evolutionary study system consisting of natural populations is minor. It is therefore promising that we are able to extract interesting results based on a relatively small sample. The method is also useful for organismal groups such as fungi, where ancient genomes cannot be retrieved due to poor fossilization (Berbee et al., 2020; ancestral populations have, for example, been detected through genomic sequencing of subfossil in a study of the giant panda; Sheng et al., 2019). Including ghost populations in modelling can improve the estimate of migration rates (Beerli, 2004; Slatkin, 2004). To increase our understanding of how introgression and gene flow affects the speciation continuum, it requires that researchers account for scenarios such as extinct lineages and ghost populations when performing model testing.

The signs of introgression observed in the oldest migration in the demographic modelling and in the *D* and *f* statistics are likely a case of introgression from extinct lineages. Ancient introgression has previously been detected from extinct cave bears in the genomes of brown bears (*Ursus arctus*; Barlow et al., 2018), through phenotype analyses of beak sizes in one of Darwin's finches (*Geospiza fortis*; Grant & Grant, 2021), and in the mitochondrial genome of the intermediate horseshoe bat (*Rhinolophus affinis*; Mao et al., 2012), to name a few. Genes or alleles from extinct lineages can therefore persist in extant species and might impose adaptive benefits (Racimo et al., 2015; The Heliconius Genome Consortium et al., 2012). It is difficult to say if this is the case with *T. abietinum* and *T. fuscoviolaceum*, but genes found in HMM outlier windows of the f_{dM} analysis may represent putatively

adaptive genes with an ancient introgression origin. Many of the genes code for proteins of unknown function, which is common in non-model organisms due to limited research. However, the genes with similarity to other functional annotated genes are involved in several different functions in organisms. For example, oxidoreductases and hydrolases partake in numerous enzymatic reactions and are known to be important for wood decaying fungi to depolymerize the recalcitrant woody substrate (Floudas et al., 2012). Nevertheless, whether any of these genes are involved in adaptive introgression cannot be concluded based on the f_{dM} analysis alone. To extrapolate any adaptive implications from the GO enrichment analysis would not be appropriate, based on the lack of significance. It is also possible that the signs of introgression observed in the f_{dM} analysis are due to non-adaptive factors. For example, parts of the genome stemming from ancient introgression can persist due to recombination and constraint (e.g., Schumer et al., 2016, 2018). Thus, this question remains inconclusive until further analyses are conducted (e.g., recombination rates along the genome). However, the retention of the introgressed regions in the genome is still interesting and acts as a detection marker for the evolutionary history of these species not revealed by examining compatibility in the current populations.

Genes transferred through introgression can lead to an expansion of a species' distribution range, as for example seen for habitat and climate adaptation in cypress species (*Cupressus* spp.; Ma et al., 2019). The divergence of many of the taxa in the family Pinaceae, which includes the current host species of *T. fuscoviolaceum* and *T. abietinum*, is dated to the Jurassic (< ~185 million years ago; Ran et al., 2018), the same period as the divergence of Hymenochaetales (Varga et al., 2019). There are several examples where research on cryptic diversity in fungi has revealed high divergence and old divergence times when species initially were thought to be closely related (summarized in Skrede, 2021), which may also be the case for *T. fuscoviolaceum* and *T. abietinum*. Our results do not conclusively show adaptive introgression but based on the large nucleotide discrepancies and most likely old divergence, one could speculate that the introgression from ancestral populations has facilitated adaption to a larger host range of *T. fuscoviolaceum* and *T. abietinum* as conifers diverged and expanded across the northern hemisphere. However, additional research (e.g., protein function analysis) is needed to say anything certain about the implications of introgression between the sister species.

Since introgression can impact the evolutionary trajectory of species, it is an important mechanism to consider when investigating the evolutionary history of taxa. Introgression is not well examined in fungi or within an experimental system based on natural populations, and historically most introgression studies have been carried out on mammals or plants (Dagilis et al., 2021). Our results indicate that ancient introgression can be detected also among divergent species. Even though the phylogenetic relationship between *T. fuscoviolaceum* and *T. abietinum* is well-defined (Peris et al., 2022; Seierstad et al., 2020), signals of introgression lingering in their genomes suggest that the evolutionary history of these species is more complex than the current phylogenies can reveal.

5 | CONCLUSION

Our study corroborates earlier findings, indicating that *T. abietinum* and *T. fuscoviolaceum* do not hybridize in vitro. Our results show that the sister species are highly divergent, exhibiting large genetic differences and are reproductively isolated. Nevertheless, introgression analyses display admixture, with small regions of introgression occurring throughout the genomes. These signs point to cases of both ancient and recent introgression between ancestral and current populations of *T. abietinum* and *T. fuscoviolaceum*, including a ghost population of a non-sampled or extinct population. Regardless of a well-resolved phylogeny, the evolutionary history of these species is intricate, including transfer of genes across lineages with unknown implications. This study builds on a small collection of studies detecting introgression between highly divergent species, expanding our knowledge on speciation and the permeability of reproductive barriers. The study also presents a novel system including natural populations and in vitro experiments, which is much needed for understanding the speciation continuum. The ceaselessness of speciation will naturally leave traces of historical events in the genomes of extant organisms. Accounting for these events when investigating speciation and adaptation can give insight into how evolution proceeds and shapes the diversity we observe today, as well as how populations are affected in the future. It will be interesting to use this fungal experimental system applying other approaches, including protein function analysis, to link introgression to historical events (e.g., host shifts) and increase insight into the mechanisms governing divergence and adaptation.

CONFLICT OF INTEREST STATEMENT

All authors declare no conflict of interest.

PEER REVIEW

The peer review history for this article is available at https://www.webofscience.com/api/gateway/wos/peer-review/10.1111/jeb.14190.

DATA AVAILABILITY STATEMENT

Illumina sequences and reference genomes are deposited in the SRA database, Bioproject PRJNA679164 (https://doi.org/10.5061/dryad.fxpnvx0t4). Datasets with VCF files are submitted to Dryad (https://doi.org/10.5061/dryad.xpnvx0kkz) and linked to at GitHub (https://zenodo.org/badge/latestdoi/619255024). The GitHub page also contains some scripts used in the analyses.

ORCID

Vilde Bruhn Kinneberg https://orcid.org/0000-0001-7077-6638
Dabao Sun Lü https://orcid.org/0000-0001-8257-307X
David Peris https://orcid.org/0000-0001-9912-8802
Mark Ravinet https://orcid.org/0000-0002-2841-1798
Inger Skrede https://orcid.org/0000-0002-1113-7403

REFERENCES

Abbott, R., Albach, D., Ansell, S., Arntzen, J. W., Baird, S. J. E., Bierne, N., Boughman, J., Brelsford, A., Buerkle, C. A., Buggs, R., Butlin, R. K., Dieckmann, U., Eroukhmanoff, F., Grill, A., Cahan, S. H., Hermansen, J. S., Hewitt, G., Hudson, A. G., Jiggins, C., … Zinner, D. (2013). Hybridization and speciation. *Journal of Evolutionary Biology*, *26*, 229–246.

Abbott, R. J., Hegarty, M. J., Hiscock, S. J., & Brennan, A. C. (2010). Homoploid hybrid speciation in action. *Taxon*, *59*, 1375–1386.

Ackermann, R. R., Arnold, M. L., Baiz, M. D., Cahill, J. A., Cortés-Ortiz, L., Evans, B. J., Grant, B. R., Grant, P. R., Hallgrimsson, B., Humphreys, R. A., Jolly, C. J., Malukiewicz, J., Percival, C. J., Ritzman, T. B., Roos, C., Roseman, C. C., Schroeder, L., Smith, F. H., Warren, K. A., … Zinner, D. (2019). Hybridization in human evolution: Insights from other organisms. *Evolutionary Anthropology*, *28*, 189–209.

Aguillon, S. M., Dodge, T. O., Preising, G. A., & Schumer, M. (2022). Introgression. *Current Biology*, *32*, R865–R868.

Alexa, A., & Rahnenfuhrer, J. (2021). *topGO: Enrichment analysis for gene ontology. R package version 2.40.* https://bioconductor.org/packages/release/bioc/html/topGO.html

Altschul, S. F., Gish, W., Miller, W., Meyers, E. W., & Lipman, D. J. (1990). Basic local alignment search tool. *Journal of Molecular Biology*, *215*, 403–410.

Anderson, E., & Hubricht, L. (1938). Hybridization in *Tradescantia*. III. The evidence for introgressive hybridization. *American Journal of Botany*, *25*, 396–402.

Andrews, S. (2010). *FastQC: A quality control tool for high throughput sequence data.* http://www.bioinformatics.babraham.ac.uk/projects/fastqc/

Barlow, A., Cahill, J. A., Hartmann, S., Theunert, C., Xenikoudakis, G., Fortes, G. G., Paijmans, J. L. A., Rabeder, G., Frischauf, C., Grandal-d'Anglade, A., García-Vázquez, A., Murtskhvaladze, M., Saarma, U., Anijalg, P., Skrbinšek, T., Bertorelle, G., Gasparian, B., Bar-Oz, G., Pinhasi, R., … Hofreiter, M. (2018). Partial genomic survival of cave bears in living brown bears. *Nature Ecology & Evolution*, *2*, 1563–1570.

Baumgartner, K., Baker, B. R., Korhonen, K., Zhao, J., Hughes, K. W., Bruhn, J., Bowman, T. S., & Bergemann, S. E. (2012). Evidence of natural hybridization among homothallic members of the basidiomycete *Armillaria mellea* sensu stricto. *Fungal Biology*, *116*, 677–691.

Beerli, P. (2004). Effect of unsampled populations on the estimation of population sizes and migration rates between sampled populations. *Molecular Ecology*, *13*, 827–836.

Bengtson, S., Rasmussen, B., Ivarsson, M., Muhling, J., Broman, C., Marone, F., Stampanoni, M., & Bekker, A. (2017). Fungus-like mycelial fossils in 2.4-billion-year-old vesicular basalt. *Nature Ecology & Evolution*, *1*, 0141.

Bengtsson, H. (2021). *R.utils: Various programming utilities. R package version 2.11.0.* https://CRAN.R-project.org/package=R.utils

Berbee, M. L., Strullu-Derrien, C., Delaux, P.-M., Strother, P. K., Kenrick, P., Selosse, M.-A., & Taylor, J. W. (2020). Genomic and fossil windows into the secret lives of the most ancient fungi. *Nature Reviews. Microbiology*, *18*, 717–730.

Bresinsky, A., Fischer, M., Meixner, B., & Paulus, W. (1987). Speciation in *Pleurotus*. *Mycologia*, *79*, 234–245.

Butlin, R. (1987). Speciation by reinforcement. *Trends in Ecology & Evolution*, *2*, 8–13.

Chang, C. C., Chow, C. C., Tellier, L. C., Vattikuti, S., Purcell, S. M., & Lee, J. J. (2015). Second generation PLINK: Rising to the challenge of larger and richer datasets. *GigaScience*, *4*, 7.

Crowl, A. A., Manos, P. S., McVay, J. D., Lemmon, A. R., Lemmon, E. M., & Hipp, A. L. (2019). Uncovering the genomic signature of ancient introgression between white oak lineages (*Quercus*). *The New Phytologist*, *226*, 1158–1170.

Cuevas, A., Eroukhmanoff, F., Ravinet, M., Sætre, G.-L., & Runemark, A. (2022). Predictors of genomic differentiation within a hybrid taxon. *PLoS Genetics*, *18*, e1010027.

Dagilis, A. J., Peede, D., Coughlan, J. M., Jofre, G. I., D'Agostino, E. R. R., Mavengere, H., Tate, A. D., & Matute, D. R. (2021). 15 years of introgression studies: Quantifying gene flow across Eukaryotes. *bioRxiv*. https://doi.org/10.1101/2021.06.15.448399

Danecek, P., Auton, A., Abecasis, G., Albers, C. A., Banks, E., DePristo, M. A., Handsaker, R., Lunter, G., Marth, G., Sherry, S. T., McVean, G., Durbin, R., & 1000 Genomes Project Analysis Group. (2011). The variant call format and VCFtools. *Bioinformatics*, *27*, 2156–2158.

Danecek, P., Bonfield, J. K., Liddle, J., Marshall, J., Ohan, V., Pollard, M. O., Whitwham, A., Keane, T., McCarthy, S. A., Davies, R. M., & Li, H. (2021). Twelve years of SAMtools and BCFtools. *GigaScience*, *10*, giab008.

Durand, E. Y., Patterson, N., Reich, D., & Slatkin, M. (2011). Testing for ancient admixture between closely related populations. *Molecular Biology and Evolution*, *28*, 2239–2252.

Durvasula, A., & Sankararaman, S. (2019). A statistical model for reference-free inference of archaic local ancestry. *PLoS Genetics*, *15*, e1008175.

Eberlein, C., Hénault, M., Fijarczyk, A., Charron, G., Bouvier, M., Kohn, L. M., Anderson, J. B., & Landry, C. R. (2019). Hybridization is a recurrent evolutionary stimulus in wild yeast speciation. *Nature Communications*, *10*, 923.

Ewels, P., Magnusson, M., Lundin, S., & Käller, M. (2016). MultiQC: Summarize analysis results for multiple tools and samples in a single report. *Bioinformatics*, 32, 3047–3048.

Excoffier, L., Marchi, N., Marques, D. A., Matthey-Doret, R., Gouy, A., & Sousa, V. C. (2021). *fastsimcoal2*: Demographic inference under complex evolutionary scenarios. *Bioinformatics*, 37, 4882–4885.

Fitak, R. R. (2021). OptM: Estimating the optimal number of migration edges on population trees using *Treemix. Biology Methods and Protocols*, 6, bpab017.

Floudas, D., Binder, M., Riley, R., Barry, K., Blanchette, R. A., Henrissat, B., Martínez, A. T., Otillar, R., Spatafora, J. W., Yadav, J. S., Aerts, A., Benoit, I., Boyd, A., Carlson, A., Copeland, A., Coutinho, P. M., de Vries, R. P., Ferreira, P., Findley, K., … Hibbett, D. S. (2012). The Paleozoic origin of enzymatic lignin decomposition reconstructed from 31 fungal genomes. *Science*, 336, 1715–1719.

Flynn, J. M., Hubley, R., Goubert, C., Rosen, J., Clark, A. G., Feschotte, C., & Smit, A. F. (2020). RepeatModeler2 for automated genomic discovery of transposable element families. *Proceedings of the National Academy of Sciences of the United States of America*, 117, 9451–9457.

Fraser, J. A., Hsueh, Y.-P., Findley, K. M., & Heitman, J. (2007). Evolution of the mating-type locus: The Basidiomycetes. In J. Heitman, J. W. Kronstad, J. W. Taylor, & L. A. Casselton (Eds.), *Sex in fungi* (pp. 19–34). ASM Press.

Garbelotto, M., Ratcliff, A., Bruns, T. D., Cobb, F. W., & Otrosina, W. J. (1996). Use of taxon-specific competitive-priming PCR to study host specificity, hybridization, and intergroup gene flow in intersterility groups of *Heterobasidion annosum. Phytopathology*, 86, 543–551.

Giordano, L., Sillo, F., Garbelotto, M., & Gonthier, P. (2018). Mitonuclear interactions may contribute to fitness of fungal hybrids. *Scientific Reports*, 8, 1706.

Grant, P. R., & Grant, B. R. (2019). Hybridization increases population variation during adaptive radiation. *Proceedings of the National Academy of Sciences of the United States of America*, 116, 23216–23224.

Grant, P. R., & Grant, B. R. (2021). Morphological ghosts of introgression in Darwin's finch populations. *Proceedings of the National Academy of Sciences of the United States of America*, 118, e2107434118.

Green, R. E., Krause, J., Briggs, A. W., Maricic, T., Stenzel, U., Kircher, M., Patterson, N., Li, H., Zhai, W. W., Fritz, M. H. Y., Hansen, N. F., Durand, E. Y., Malaspinas, A. S., Jensen, J. D., Marques-Bonet, T., Alkan, C., Prufer, K., Meyer, M., Burbano, H. A., … Pääbo, S. (2010). A draft sequence of the Neandertal genome. *Science*, 328, 710–722.

Harrison, R. G., & Larson, E. L. (2014). Hybridization, introgression, and the nature of species boundaries. *The Journal of Heredity*, 105, 795–809.

Harte, D. (2021). *HiddenMarkov: Hidden Markov Models. R package version 1.8-13*. Statistics Research Associates. https://cran.r-project.org/web/packages/HiddenMarkov/index.html

Hegarty, M. J., & Hiscock, S. J. (2005). Hybrid speciation in plants: New insights from molecular studies. *The New Phytologist*, 165, 411–423.

Heinzelmann, R., Rigling, D., Sipos, G., Münsterkötter, M., & Croll, D. (2020). Chromosomal assembly and analyses of genome-wide recombination rates in the forest pathogenic fungus *Armillaria ostoyae. Heredity*, 124, 699–713.

Hermansen, J. S., Sæther, S. A., Elgvin, T. O., Borge, T., Hjelle, E., & Sætre, G.-P. (2011). Hybrid speciation in sparrows I: Phenotypic intermediacy, genetic admixture and barriers to gene flow. *Molecular Ecology*, 20, 3812–3822.

Holt, C., & Yandell, M. (2011). MAKER2: An annotation pipeline and genome-database management tool for second-generation genome projects. *BMC Bioinformatics*, 12, 491.

Index Fungorum. (2021). *Index Fungorum, The Royal Botanic Gardens Kew.* www.indexfungorum.org

Jain, C., Rodriguez-R, L. M., Phillippy, A. M., Konstantinidis, K. T., & Aluru, S. (2018). High throughput ANI analysis of 90 K prokaryotic genomes reveals clear species boundaries. *Nature Communications*, 9, 5114.

James, T. Y., Kües, U., Rehnerc, S. A., & Vilgalysa, R. (2004). Evolution of the gene encoding mitochondrial intermediate peptidase and its cosegregation with the A mating-type locus of mushroom fungi. *Fungal Genetics and Biology*, 41, 381–390.

Jones, P., Binns, D., Chang, H.-Y., Fraser, M., Li, W., McAnulla, C., McWilliam, H., Maslen, J., Mitchell, A., Nuka, G., Pesseat, S., Quinn, A. F., Sangrador-Vegas, A., Scheremetjew, M., Yong, S.-Y., Lopez, R., & Hunter, S. (2014). InterProScan 5: Genome-scale protein function classification. *Bioinformatics*, 30, 1236–1240.

Kauserud, H., & Schumacher, T. (2003). Ribosomal DNA variation, recombination and inheritance in the basidiomycete *Trichaptum abietinum*: Implications for reticulate evolution. *Heredity*, 91, 163–172.

Keuler, R., Garretson, A., Saunders, T., Erickson, R. J., St Andre, N., Grewe, F., Smith, H., Lumbsch, H. T., Huang, J. P., St Clair, L. L., & Leavitt, S. D. (2020). Genome-scale data reveal the role of hybridization in lichen-forming fungi. *Scientific Reports*, 10, 1497.

Ko, K. S., & Jung, H. S. (2002). Three nonorthologous ITS1 types are present in a polypore fungus *Trichaptum abietinum. Molecular Phylogenetics and Evolution*, 23, 112–122.

Krueger, F. (2015). *Trim Galore!: A wrapper tool around Cutadapt and FastQC to consistently apply quality and adapter trimming to FastQ files.* http://www.bioinformatics.babraham.ac.uk/projects/trim_galore/

Langdon, Q. K., Peris, D., Baker, E. C. P., Opulente, D. A., Nguyen, H.-V., Bond, U., Gonçalves, P., Sampaio, J. P., Libkind, D., & Hittinger, C. T. (2019). Fermentation innovation through complex hybridization of wild and domesticated yeasts. *Nature Ecology & Evolution*, 3(1576), 1586.

Langdon, Q. K., Peris, D., Kyle, B., & Hittinger, C. T. (2018). sppIDer: A species identification tool to investigate hybrid genomes with high-throughput sequencing. *Molecular Biology and Evolution*, 35, 2835–2849.

Lawrence, M., Gentleman, R., & Carey, V. (2009). rtracklayer: An R package for interfacing with genome browsers. *Bioinformatics*, 25, 1841–1842.

Li, H., & Durbin, R. (2009). Fast and accurate short read alignment with Burrows–Wheeler Transform. *Bioinformatics*, 25, 1754–1760.

Li, H., Handsaker, B., Wysoker, A., Fennell, T., Ruan, J., Homer, N., Marth, G., Abecasis, G., Durbin, R., & 1000 Genome Project Data Processing Subgroup. (2009). The sequence alignment/map (SAM) format and SAMtools. *Bioinformatics*, 25, 2078–2079.

Li, Y., Steenwyk, J. L., Chang, Y., Wang, Y., James, T. Y., Stajich, J. E., Spatafora, J. W., Groenewald, M., Dunn, C. W., Hittinger, C. T., Shen, X.-X., & Rokas, A. (2021). A genome scale phylogeny of the kingdom fungi. *Current Biology*, 31, 1653–1665.e5.

Lunter, G., & Goodson, M. (2011). Stampy: A statistical algorithm for sensitive and fast mapping of Illumina sequence reads. *Genome Research*, 21, 961–973.

Ma, Y., Wang, J., Hu, Q., Li, J., Sun, Y., Zhang, L., Abbott, R. J., Liu, J., & Mao, L. (2019). Ancient introgression drives adaptation to cooler and drier mountain habitats in a cypress species complex. *Communications Biology*, 2, 213.

Macrae, R. (1967). Pairing incompatibility and other distinctions among *Hirchiporus abietinus*, *H. fusco-violaceus*, and *H. laricinus. Canadian Journal of Botany*, 45, 1371–1399.

Magasi, L. P. (1976). Incompatibility factors in *Polyporus abietinus*, their numbers and distribution. *Memoirs of the New York Botanical Garden*, 28, 163–173.

Malinsky, M., Challis, R. J., Alexandra, M. T., Schiffels, S., Terai, Y., Ngatunga, P. B., Miska, E. A., Durbin, R., Genner, M. J., & Turner, G. F. (2015). Genomic islands of speciation separate cichlid ecomorphs in an East African crater lake. *Science*, 350, 1493–1498.

Mallet, J., Besansky, N., & Hahn, M. W. (2016). How reticulated are species? *BioEssays*, 38, 140–149.

Mao, X., He, G., Hua, P., Jones, G., Zhang, S., & Rossiter, S. J. (2012). Historical introgression and the persistence of ghost alleles in the intermediate horseshoe bat (*Rhinolophus affinis*). *Molecular Ecology*, *22*, 1035–1050.

Martin, S. H., Davey, J. W., & Jiggins, C. D. (2014). Evaluating the use of ABBA–BABA statistics to locate introgressed loci. *Molecular Biology and Evolution*, *32*, 244–257.

Martin, S. H., Davey, J. W., Salazar, C., & Jiggins, C. D. (2019). Recombination rate variation shapes barriers to introgression across butterfly genomes. *PLoS Biology*, *17*, e2006288.

Mavárez, J., Salazar, C. A., Bermingham, E., Salcedo, C., Jiggins, C. D., & Linares, M. (2006). Speciation by hybridization in *Heliconius* butterflies. *Nature*, *441*, 868–871.

May, G., Shaw, F., Badrane, H., & Vekemans, X. (1999). The signature of balancing selection: Fungal mating compatibility gene evolution. *Proceedings of the National Academy of Sciences of the United States of America*, *96*, 9172–9177.

Maxwell, C. S., Sepulveda, V. E., Turissini, D. A., Goldman, W. E., & Matute, D. R. (2018). Recent admixture between species of the fungal pathogen Histoplasma. *Evolution Letters*, *2*(3), 210–220.

McKenna, A., Hanna, H., Banks, E., Sivachenko, A., Cibulskis, K., Kernytsky, A., Garimella, K., Altshuler, D., Gabriel, S., Daly, M., & DePristo, M. A. (2010). The Genome Analysis Toolkit: A MapReduce framework for analyzing next-generation DNA sequencing data. *Genome Research*, *20*, 1297–1303.

Minh, B. Q., Schmidt, H. A., Chernomor, O., Schrempf, D., Woodhams, M. D., von Haeseler, A., & Lanfear, R. (2020). IQ-TREE 2: New models and efficient methods for phylogenetic inference in the genomic era. *Molecular Biology and Evolution*, *37*, 1530–1534.

Moore, D., Robson, G. D., & Trinci, A. P. J. (2011). Chapter 12.14 – Classic genetic approaches to study development and the impact of genomic data mining. In D. Moore, G. D. Robson, & A. P. J. Trinci (Eds.), *21st century guidebook to fungi* (pp. 311–315). Cambridge University Press.

Nachman, M. W., & Payseur, B. A. (2012). Recombination rate variation and speciation: Theoretical predictions and empirical results from rabbits and mice. *Philosophical Transactions of the Royal Society of London. Series B, Biological Sciences*, *367*, 409–421.

Nei, M., Maruyama, T., & Wu, C.-I. (1983). Models of evolution of reproductive isolation. *Genetics*, *103*, 557–579.

Nelson, T. C., Stathos, A. M., Vanderpool, D. D., Finseth, F. R., Yuan, Y.-W., & Fishman, L. (2021). Ancient and recent introgression shape the evolutionary history of pollinator adaptation and speciation in a model monkeyflower radiation (Mimulus section Erythranthe). *PLoS Genetics*, *17*, e1009095.

Neuwirth, E. (2014). *RColorBrewer: ColorBrewer palettes. R package version 1.1-2.* https://CRAN.R-project.org/package=RColorBrewer

Nosil, P., Feder, J. L., Flaxman, S. M., & Gompert, Z. (2017). Tipping points in the dynamics of speciation. *Nature Ecology & Evolution*, *1*, 1.

Patterson, N., Moorjani, P., Luo, Y., Mallick, S., Rohland, N., Zhan, Y., Genschoreck, T., Webster, T., & Reich, D. (2012). Ancient admixture in human history. *Genetics*, *192*, 1065–1093.

Patterson, N., Price, A. L., & Reich, D. (2006). Population structure and eigenanalysis. *PLoS Genetics*, *2*, 2074–2093.

Peris, D., Lu, D., Kinneberg, V. B., Methlie, I.-S., Dahl, M. S., James, T. Y., Kauserud, H., & Skrede, I. (2022). Large-scale fungal strain sequencing unravels the molecular diversity in mating loci maintained by long-term balancing selection. *PLoS Genetics*, *18*, e1010097.

Petr, M., Vernot, B., & Kelso, J. (2019). admixr—R package for reproducible analyses using ADMIXTOOLS. *Bioinformatics*, *35*, 3194–3195.

Pickrell, J. K., & Pritchard, J. K. (2012). Inference of population splits and mixtures from genome wide allele frequency data. *PLoS Genetics*, *8*, e1002967.

Platt, R. N., II, McDew-White, M., Clec'h, W. L., Chevalier, F. D., Allan, F., Emery, A. M., Garba, A., Hamidou, A. A., Ame, S. M., Webster, J. P., Rollinson, D., Webster, B. L., & Anderson, T. J. C. (2019). Ancient hybridization and adaptive introgression of an invadolysin gene in schistosome parasites. *Molecular Biology and Evolution*, *36*, 2127–2142.

Price, A. L., Patterson, N. J., Plenge, R. M., Weinblatt, M. E., Shadick, N. A., & Reich, D. (2006). Principal components analysis corrects for stratification in genome-wide association studies. *Nature Genetics*, *38*, 904–909.

R Core Team. (2020). *R: A language and environment for statistical computing*. R Foundation for Statistical Computing. https://www.R-project.org/

Racimo, F., Sankararaman, S., Nielsen, R., & Huerta-Sánchez, E. (2015). Evidence for archaic adaptive introgression in humans. *Nature Reviews. Genetics*, *16*, 359–371.

Raghavan, M., Skoglund, P., Graf, K., Metspalu, M., Albrechtsen, A., Moltke, I., Rasmussen, S., Stafford, T. W., Jr., Orlando, L., Metspalu, E., Karmin, M., Tambets, K., Rootsi, S., Mägi, R., Campos, P. F., Balanovska, E., Balanovsky, O., Khusnutdinova, E., Litvinov, S., … Willerslev, E. (2014). Upper Palaeolithic Siberian genome reveals dual ancestry of Native Americans. *Nature*, *505*, 87–91.

Ram, K., & Wickham, H. (2018). *wesanderson: A Wes Anderson palette generator. R package version 0.3.6.* https://CRAN.R-project.org/package=wesanderson

Ran, J.-H., Shena, T.-T., Wu, H., Gong, X., & Wang, X.-Q. (2018). Phylogeny and evolutionary history of Pinaceae updated by transcriptomic analysis. *Molecular Phylogenetics and Evolution*, *129*, 106–116.

Ravinet, M., Yoshida, K., Shigenobu, S., Toyoda, A., Fujiyama, A., & Kitano, J. (2018). The genomic landscape at a late stage of stickleback speciation: High genomic divergence interspersed by small localized regions of introgression. *PLoS Genetics*, *14*, e1007358.

Reich, D., Thangaraj, K., Patterson, N., Price, A. L., & Singh, L. (2009). Reconstructing Indian population history. *Nature*, *461*, 489–494.

Reich, D. N., Patterson, M., Kircher, F., Delfin, M. R., Nandineni, I., Pugach, A. M.-S., Ko, Y. C., Ko, T. A., Jinam, M. E., Phipps, N., Saitou, A., Wollstein, M., Kayser, S. P., & Stoneking, M. (2011). Denisova admixture and the first modern human dispersals into Southeast Asia and Oceania. *American Journal of Human Genetics*, *89*, 516–528.

Schumer, M., Cui, R., Powell, D. L., Rosenthal, G. G., & Andolfatto, P. (2016). Ancient hybridization and genomic stabilization in a swordtail fish. *Molecular Ecology*, *25*, 2661–2679.

Schumer, M., Xu, C., Powell, D. L., Durvasula, A., Skov, L., Holland, C., Blazier, J. C., Sankararaman, S., Andolfatto, P., Rosenthal, G. G., & Przeworski, M. (2018). Natural selection interacts with recombination to shape the evolution of hybrid genomes. *Science*, *360*, 656–660.

Seierstad, K. S., Fossdal, R., Miettinen, O., Carlsen, T., Skrede, I., & Kauserud, H. (2020). Contrasting genetic structuring in the closely related basidiomycetes *Trichaptum abietinum* and *Trichaptum fuscoviolaceum* (Hymenochaetales). *Fungal Biology*, *124*, 269–275.

Sheng, G.-L., Basler, N., Ji, X.-P., Paijmans, J. L. A., Alberti, F., Preick, M., Hartmann, S., Westbury, M. V., Yuan, J.-X., Jablonski, N. G., Xenikoudakis, G., Hou, X.-D., Xiao, B., Liu, J.-H., Hofreiter, M., Lai, X.-L., & Barlow, A. (2019). Paleogenome Reveals Genetic Contribution of Extinct Giant Panda to Extant Populations. *Current Biology*, *29*(10), 1695–1700.e6.

Skrede, I. (2021). Chapter one – Diversity and distribution of ligninolytic fungi. In M. Morel-Rouhier & R. Sormani (Eds.), *Advances in botanical research, vol 99: Wood degradation and ligninolytic fungi* (pp. 1–36). Academic Press.

Slatkin, M. (2004). Seeing ghosts: The effect of unsampled populations on migration rates estimated for sampled populations. *Molecular Ecology*, *14*, 67–73.

Smit, A. F. A., Hubley, R., & Green, P. (2013–2015). *RepeatMasker Open-4.0.* http://www.repeatmasker.org

Stankowski, S., & Ravinet, M. (2021). Defining the speciation continuum. *Evolution*, *75*, 1256–1273.

Stenlid, J., & Karlsson, J.-O. (1991). Partial intersterility in *Heterobasidion annosum*. *Mycological Research*, 95, 1153–1159.

Stukenbrock, E. H. (2016). The role of hybridization in the evolution and emergence of new fungal plant pathogens. *Phytopathology*, 106, 104–112.

Stukenbrock, E. H., Christiansen, F. B., Hansen, T. T., Dutheil, J. Y., & Schierup, M. H. (2012). Fusion of two divergent fungal individuals led to the recent emergence of a unique widespread pathogen species. *Proceedings of the National Academy of Sciences of the United States of America, 109*, 10954–10959.

The Heliconius Genome Consortium, Dasmahapatra, K. K., Walters, J., Briscoe, A. D., Davey, J. W., Whibley, A., Nadeau, N. J., Zimin, A. V., Hughes, D. S. T., Ferguson, L. C., Martin, S. H., Salazar, C., Lewis, J. J., Adler, S., Ahn, S.-J., Baker, D. A., Baxter, S. W., Chamberlain, N. L., Chauhan, R., ... Jiggins, C. D. (2012). Butterfly genome reveals promiscuous exchange of mimicry adaptations among species. *Nature, 487*, 94–98.

The UniProt Consortium. (2021). UniProt: The universal protein knowledgebase in 2021. *Nucleic Acids Research, 49*, D480–D489.

Van Rossum, G., & Drake, F. L. (2009). *Python 3 reference manual.* CreateSpace.

Varga, T., Krizsán, K., Földi, C., Dima, B., Sánchez-García, M., Sánchez-Ramírez, S., Szöllősi, G. J., Szarkándi, J. G., Papp, V., Albert, L., Andreopoulos, W., Angelini, C., Antonín, V., Barry, K. W., Bougher, N. L., Buchanan, P., Buyck, B., Bense, V., Catcheside, P., ... Nagy, L. G. (2019). Megaphylogeny resolves global patterns of mushroom evolution. *Nature Ecology & Evolution, 3*, 668–678.

Vlasák, J., & Vlasák, J., Jr. (2017). *Trichaptum* (Basidiomycota) in tropical America: A sequence study. *Mycosphere, 8*, 1217–1227.

Wang, G. D., Zhai, W., Yang, H. C., Wang, L., Zhong, L., Liu, Y. H., Fan, R. X., Yin, T. T., Zhu, C. L., Poyarkov, A. D., Irwin, D. M., Hytönen, M. K., Lohi, H., Wu, C. I., Savolaine, P., & Zhang, Y. P. (2016). Out of southern East Asia: The natural history of domestic dogs across the world. *Cell Research, 26*, 21–33.

Watterson, G. A. (1985). The genetic divergence of two populations. *Theoretical Population Biology, 27*, 298–317.

White, N. J., Snook, R. R., & Eyres, I. (2019). The past and future of experimental speciation. *Trends in Ecology & Evolution, 35*, 10–21.

Wickham, H. (2016). *ggplot2: Elegant graphics for data analysis* (2nd ed.). Springer.

Wickham, H., Averick, M., Bryan, J., Chang, W., McGowan, L. D., François, R., Grolemund, G., Hayes, A., Henry, L., Hester, J., Kuhn, M., Pedersen, T. L., Miller, E., Bache, S. M., Müller, K., Ooms, J., Robinson, D., Seidel, D. P., Spinu, V., ... Yutani, H. (2019). Welcome to the tidyverse. *Journal of Open Source Software, 4*, 1686.

Wood, T. E., Takebayashi, N., Barker, M. S., Mayrose, I., Greenspoon, P. B., & Rieseberg, L. H. (2009). The frequency of polyploid speciation in vascular plants. *Proceedings of the National Academy of Sciences of the United States of America, 106*, 13875–13879.

Zhang, W., Dasmahapatra, K. K., Mallet, J., Moreira, G. R. P., & Kronforst, M. R. (2016). Genome wide introgression among distantly related *Heliconius* butterfly species. *Genome Biology, 17*, 25.

SUPPORTING INFORMATION

Additional supporting information can be found online in the Supporting Information section at the end of this article.

How to cite this article: Kinneberg, V. B., Lü, D. S., Peris, D., Ravinet, M., & Skrede, I. (2023). Introgression between highly divergent fungal sister species. *Journal of Evolutionary Biology, 36*, 1133–1149. https://doi.org/10.1111/jeb.14190